Supplementary Material

Serum Amyloidogenic Nanoplaques and Cytokines in Alzheimer's Disease: Pilot Study in a Small Naturalistic Memory Clinic Cohort

Background on Time-Resolved Thioflavin T (ThT) Fluorescence Intensity Fluctuation Measurements and Analysis

Our approach brings together: 1) the high sensitivity and specificity of Thioflavin T (ThT), a benzothiazole dye that selectively binds to amyloidogenic structured protein aggregates enriched in β-sheet secondary structure, hereafter called nanoplaques, and exhibits upon binding a strong increase in fluorescence quantum yield and a shift of excitation spectrum to longer wavelengths, with 2) time-resolved fluorescence intensity fluctuation measurements in a sub-femtoliter observation volume element (OVE), to enable the detection of ThT-active structured amyloidogenic aggregates with single-molecule sensitivity [1]. To generate the miniscule OVE, the confocal optical arrangement in an epifluorescence microscope is being used. Specifically, a high numerical aperture (NA) objective is used to sharply focus the incident laser light into the sample. Fluorescence from the sample is collected by the same objective and the volume from which the signal is being detected is reduced by placing a pinhole in the optically conjugate plane in front of the detector, thus minimizing the contribution of out-of-focus light. The advantage of performing fluorescence intensity measurements in a sub-femtoliter OVE over conventional fluorescence spectroscopy measurements in the bulk, lies in the significant reduction of the number of molecules from which the background signal originates. Consequently, correlated fluctuations of emitted light coming from a single molecule/nanoparticle can be seen over the average fluorescence intensity to which many natively fluorescent molecules in the serum contribute. And, the passage of a bright ThT-active nanoplaque particle through the minute OVE can be readily discerned from the background (Supplementary Figure 1).

Time-resolved ThT fluorescence intensity fluctuation measurements and data analysis by temporal autocorrelation reveal that the average diffusion time (τ_D) of molecules in serum, when nanoplaque passage is not observed, is $\tau_D = (150 \pm 50)$ μs (Supplementary Figure 1b and c, light green). When a bright nanoplaque passes through the OVE, a pronounced peak in fluorescence intensity is observed in the time series (Supplementary Figure 1a, green) and a second component with a significantly longer diffusion time is observed in the ACC (Supplementary Figure 1b and c, dark green). The width of the fluorescence intensity peak reflects the diffusion time (τ_D), which

is related to nanoplaque size. Given that a small number of nanoplaques is observed in an individual serum sample, data from all patients in a group are pulled to have better statistics.

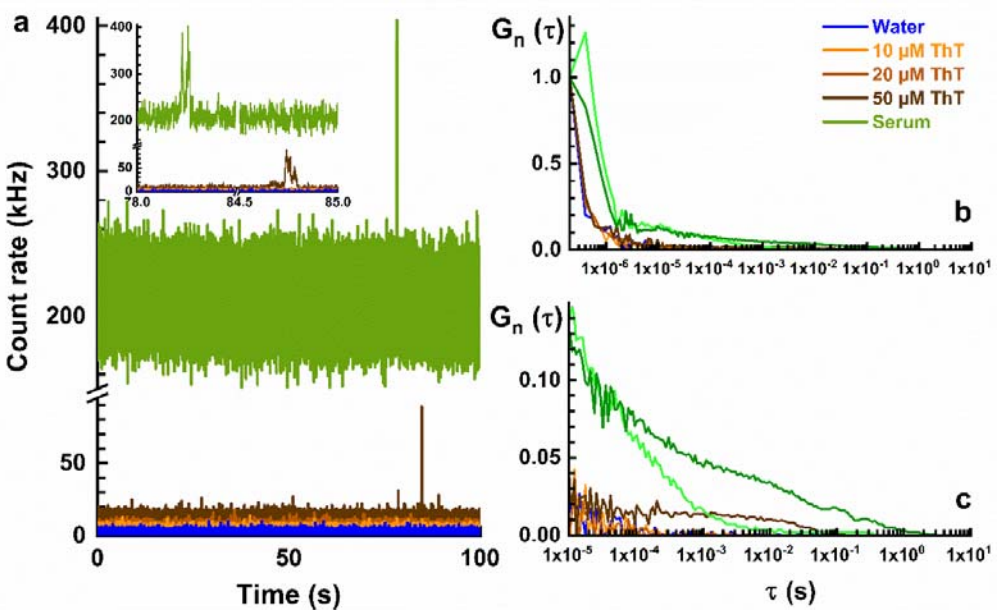

Supplementary Figure 1. Time-resolved fluorescence intensity fluctuations and corresponding autocorrelation curves (ACCs). a) Time-resolved fluorescence intensity fluctuation recorded over time in: serum with ThT (green), pure water (blue), 10 μM ThT in water (okra), 20 μM ThT in water (brown), and 50 μM ThT in water (dark brown). *Inset:* Magnified fluorescence intensity bursts shown in a. b) Corresponding temporal ACCs normalized to the same amplitude, $G(\tau) = 1$ at $\tau = 0.2$ μs. c) Magnified ACCs shown in b.

In order to ascertain that the fluorescence bursts do not reflect random events, such as electrical disturbances or passage of bright ThT micelles through the OVE, but rather the passage of ThT-active nanoplaques, control measurements were performed in water (Supplementary Figure 1, blue), 10 μM ThT in water (Supplementary Figure 1, okra), 20 μM ThT in water (Supplementary Figure 1, brown), and 50 μM ThT in water (Supplementary Figure 1, dark brown). As can be seen, correlated signal is not observed in water, 10 μM ThT, and 20 μM ThT (Supplementary Figure 1; blue, okra, and brown, respectively). In contrast, in 50 μM ThT in water, correlated signal due to formation of ThT micelles is clearly observed (Supplementary Figure 1, dark brown). Furthermore, correlation between duplicate measurements (Supplementary Figure 2) shows that the best fitting line (black) marginally differs from the line of equality ($y = x$, green), which would not be the case if the detected events were random. However, the scatter around the best fitting line, as reflected by the Pearson's correlation coefficient $r = 0.60$, indicates that inclusion of triplicate measurements or longer signal acquisition times would improve the precision by which the f_{SEO} is determined.

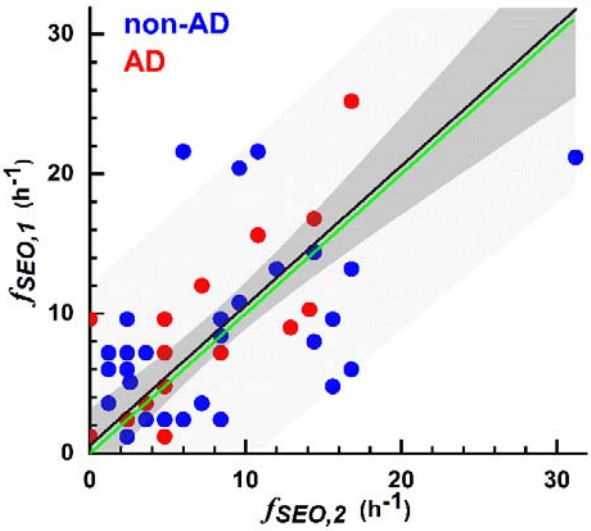

Supplementary Figure 2. Degree of association between duplicate measurements. The best fitting line (y = - 0.7 + x, black) marginally differs from the line of equality ($y = x$, green). The Pearson's correlation coefficient, r = 0.60, indicates that while there is a high degree of correlation between duplicate measurements, there is also a sizable scatter. The 95 % confidence band (grey). The 95 % prediction band (light grey).

The data in Supplementary Figure 2 show that there is no statistically significant difference in the f_{SEO} between the AD and non-AD groups, which can also be seen from the histograms of f_{SEO} spreads shown in Supplementary Figure 3.

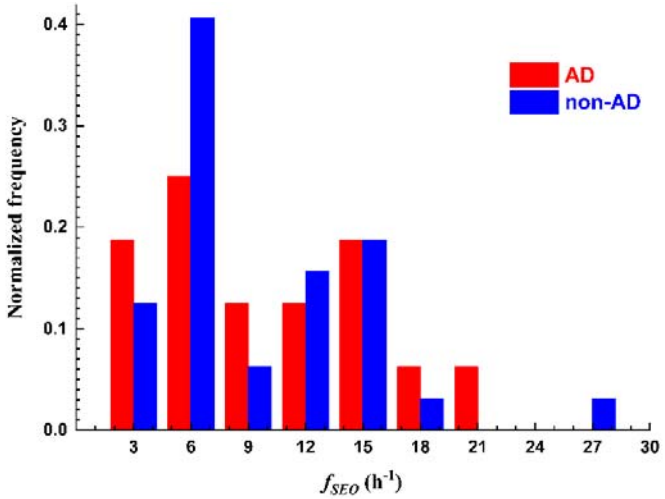

Supplementary Figure 3. Normalized histograms showing f_{SEO} spreads in the AD and non-AD groups.

Finally, while we have not observed any sedimented nanoplaques in serum, we have examined using time-resolved ThT fluorescence intensity fluctuation analysis and Confocal Laser Scanning Fluorescence Microscopy (CLSM) how the concentration of nanoplaques, as reflected by the average number of molecules in the OVE (N), their size, as reflected by the diffusion time (τ_D), brightness, as reflected by the counts *per* molecule *per* second (CPMS), and sedimentation, as

reflected by CLSM imaging, are changing over time during 10 μM $A\beta_{1-42}$ aggregation (Supplementary Figure 4). From this analysis, the intricate nanoplaque formation and sedimentation dynamics can be gleaned.

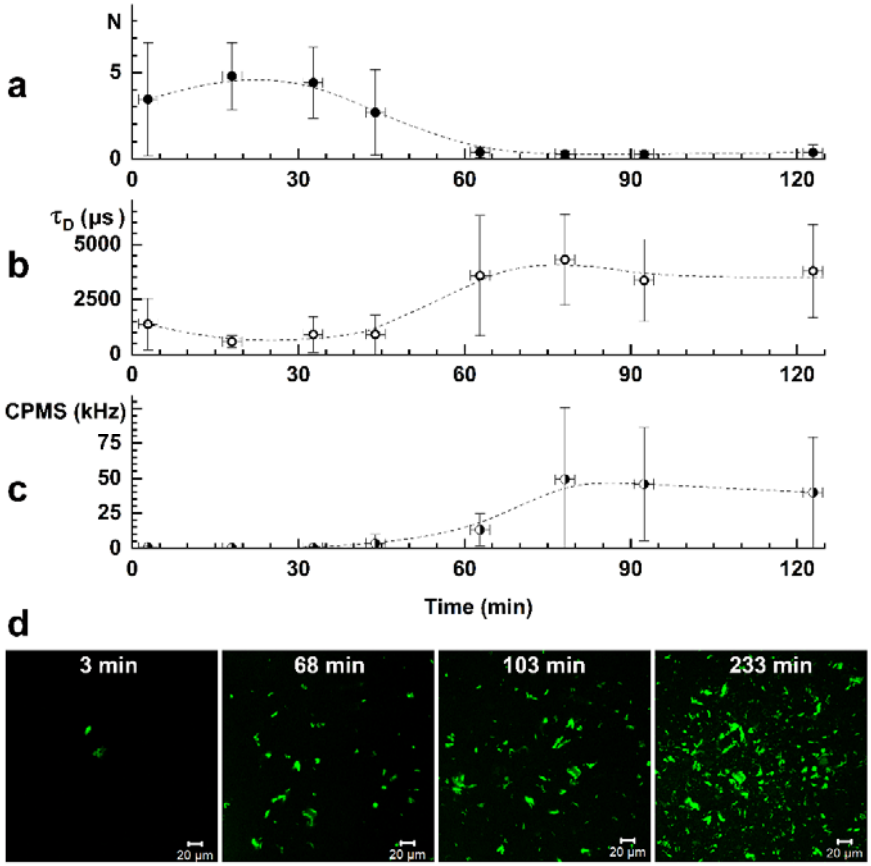

Supplementary Figure 4. The complex dynamics of $A\beta_{1-42}$ aggregation and sedimentation in a 10 μM $A\beta_{1-42}$ solution. a) Change in the average number of nanoplaques (N) over time. b) Change in the average diffusion time (τ_D), which correlates with the size of nanoplaques. c) Change in the average brightness of nanoplaques over time. The dashed lines in a-c are b-spline interpolation curves added to help guide the eye. It is important to note that the large error bars in a-c reflect sample heterogeneity rather than method imprecision. d) CLSM images showing how the concentration and size of sedimented $A\beta_{1-42}$ plaques is changing over time.

REFERENCE

[1] Tiiman A, Jelić V, Jarvet J, Järemo P, Bogdanović N, Rigler R, Terenius L, Gräslund A, Vukojević V (2019) Amyloidogenic nanoplaques in blood serum of patients with Alzheimer's disease revealed by time-resolved Thioflavin T fluorescence intensity fluctuation analysis. *J Alzheimers Dis* **68**, 571-582.

Supplementary Results

Supplementary Table 1. Number of A+ (amyloid positive), T+ (tau positive) and N+ (neurodegeneration positive) patients in the AD and non-AD groups.

	Non-AD (13)	AD (13)
A+	1 (7.7 %)	12 (92.3 %)
T+	0 (0.0 %)	5 (38.5 %)
N+	1 (7.7 %)	9 (69.2 %)

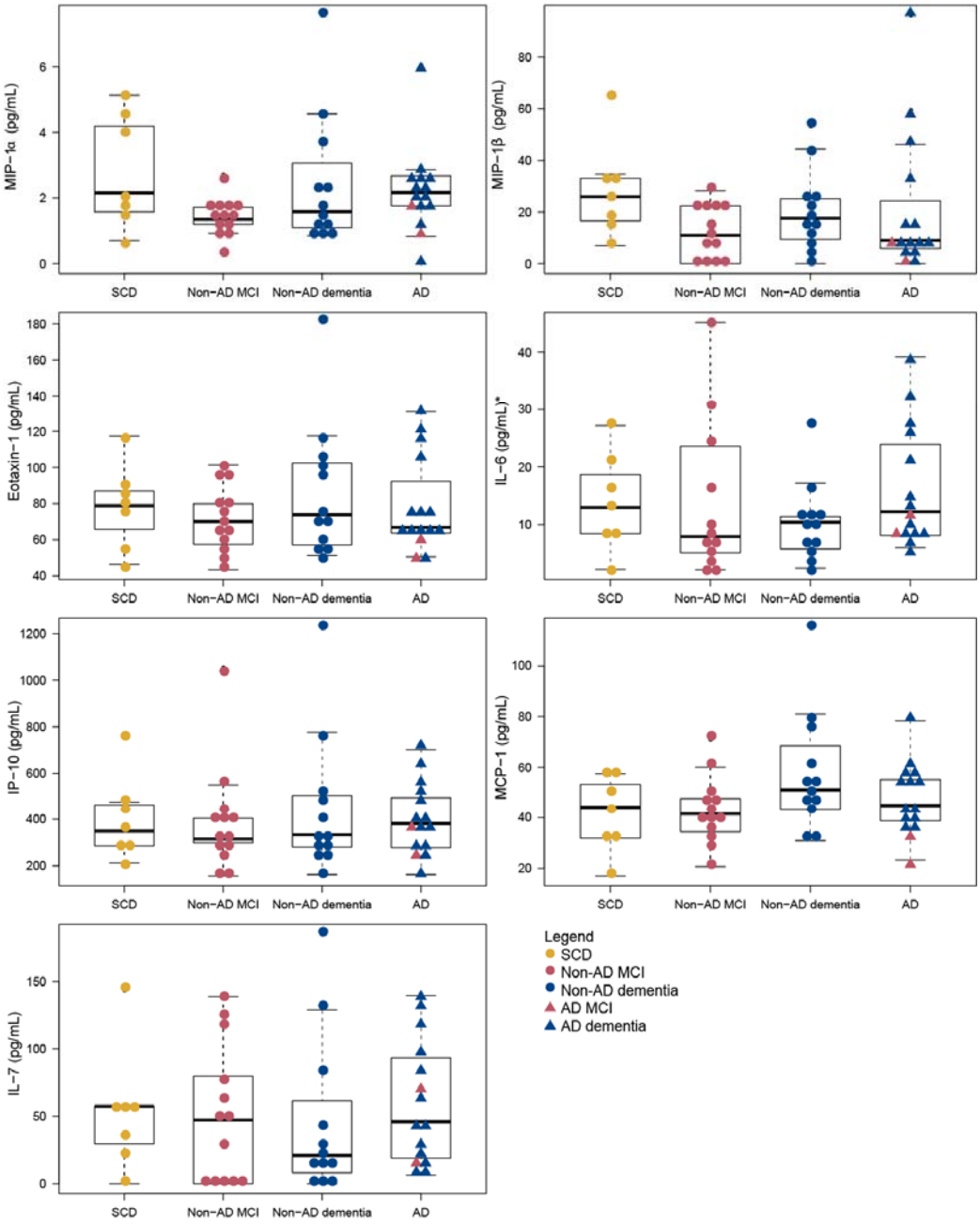

Supplementary Figure 5. Distribution of seven serum cytokines across SCD, Non-AD MCI, Non-AD dementia and AD (MCI and dementia). AD, Alzheimer's disease; IL, interleukin; IP, interferon gamma-induced protein; MCI, mild cognitive impairment; MCP, monocyte chemoattractant protein; MIP, macrophage inflammatory protein; SCD, subjective cognitive decline.